DOI: https://doi.org/10.24113/ijoscience.v7i1.345

Transient Stability Improvement Analysis of DFIG Based Variable Speed Wind Generator Using IGBT- Bridge-Type Fault Current Limiter

Roshan Brahmwanshi
M. Tech Scholar
Scope College of Engineering
Bhopal (MP), India
roshan.brahmwanshi@gmail.com

Eknath Borkar
Associate Professor
Scope College of Engineering
Bhopal (MP), India
bhaskarbharat71@gmail.com

Abstract: **Due to its many advantages such as the improved power quality, high energy efficiency and controllability, etc. the variable speed wind turbine using a doubly fed induction generator (DFIG) is becoming a popular concept and thus the modeling of the DFIG based wind turbine and improvement in the transient fault conditions is an important consideration. In this paper, Transient stability improvement has been done by using Superfluous Fault Current Limiter [SFCL]. A new design of SFCL IGBT- Bridge-type SFCL shunted with a variable resistor Rsh has been proposed. Rsh is modeled to decrease the terminal Voltage deviation to minimum level by reducing the amount of current at the bus terminal. Comparison of Voltage deviation and current deviation with the resistive type SFCL and IGBT- bridge-type SFCL show considerable decrease in both quantities by using IGBT- bridge-type SFCL. The values of Voltage deviation at the bus terminal is 8.223 e-8 % for proposed SFCL which is less than the resistive type SFCL that is, 14.4 e^{-8} %. The huge Voltage sag has been considerably reduced by reduction of high level of current to 0.0004401 % in IGBT-bridge-Type SFCL from 0.0004624% in resistive type SFCL. Thus proposed SFCL has caused significant improvement in transient stability keeping the deviation in active and reactive power during faults to minimum level.**

Keywords: SFCL, DFIG, PCC, MATLAB.

I. INTRODUCTION

Renewable energies have the potential to reduce pollution, slow global warming and create new industries and jobs. There are huge economic opportunities for countries that invent, produce and export clean energy technologies. The use of renewable energies has become a global research and development problem. Wind power is one of the fastest growing renewable technologies and has the potential to meet a significant portion of our electricity needs. It is now also considered an energy source that allows electricity to be produced with minimal environmental disturbance. In recent years, dual-fuel induction generators (DFIGs) have been one of the most used large grid-connected wind turbines. They are becoming more and more acceptable due to their suitability for variable speed wind turbines and are more attractive than fixed speed systems due to their efficient power generation, better power quality and performance. Performance of electronic devices, which carry only a fraction of the total power. (20-30%).

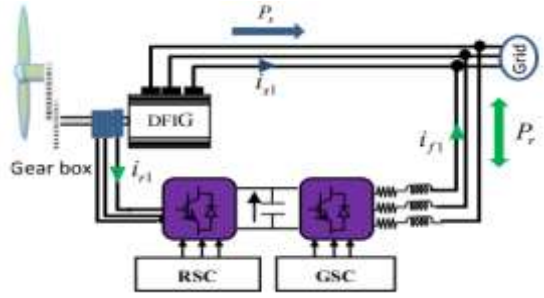

Fig. 1 Schematic diagram of a DFIG.

II. LITERATURE REVIEW

M. A. Chowdhury et al. [1] This article presents a complete and aggregated wind farm model with a dual power induction generator (DFIG). The simulations were performed and compared for the two models in order to demonstrate the efficiency of the aggregate model in terms of precision in approximating the collective dynamic responses to the common connection point (PCC) and in reducing the computation time of the simulation.

J. Wang et al. [2] This article uses hierarchical grouping methods to classify the wind farm, performs hierarchical cluster analysis for all wind turbines, and divides it into multiple clusters using the transient Voltage properties of each wind turbine as the cluster target. A concentrated process, which uses the actual

performance characteristics of the cluster as a benchmark, manages the identification of the parameters. The first WTG models, which are mainly based on electromagnetic transient models and contain many power electronic components, are complex and have low convergence and low computation speed.

Y. Lei et al. [3] in this paper, a simple DFIG wind turbine model is developed in which the converter is simulated as a controlled Voltage source and the rotor current is adjusted to satisfy the active and reactive power generation command. The performance and accuracy of the model were also compared with the detailed model developed by DIgSILENT.

Z. Zhao et al. [4] In this article, taking into account the problem of wind speed difference due to complex terrain and irregularly arranged wind farms in large wind farms, measurement data on a long-term scale is selected as a cluster-dependent index. The simulation results show that the equivalent dynamic model of the created wind farm can accurately reflect the dynamic nature at the common coupling point (PCC).

III. OBJECTIVE

Transient stability enhancement analysis of the doubly fed induction generator–based variable speed wind generator is being performed among the most promising series compensating devices like Resistive type fault current limiter and IGBT – bridge type SFCL with shunted resistor.

The main objectives are:

(i) Comparison of Voltage deviation, current deviation generated in the DFIG model while using Resistive Type SFCL and IGBT- bridge type SFCL as compensating devices.

(ii) To enhance the transient stability of the DFIG system for both the symmetrical and asymmetrical faults more efficiently than the DC Resistive type SFCL.

(iii) To reduce huge Voltage sag and high level of current in the DFIG based model and hence reduce the power losses in the system thereby improving the efficiency and reliability.

(iv) Comparison of power deviation in DFIG model without using SFCL, With Resistive type SFCL and IGBT-Bridge-type SFCL.

IV. METHODOLOGY

A. *DFIG Modeling*

2 MW/690V Wind Farm has been modeled in MATLAB/ SIMULINK. Figure 2. Mechanically the wind turbine is coupled to the Doubly Fed Induction Generator (DFIG) through a gear box. The step up transformer connects the generator to infinite bus bar at bus B1.

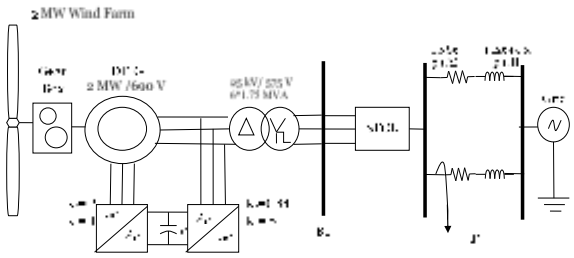

Fig. 2 Wind Turbine Test Model

In modeling of turbine model, we consider the most common relationship between the wind speed and the extracted mechanical power P_{wind} by the wind turbine, which can be defined as follows

$$P_{wind} = 0.5\ \rho\ C_p\ (\lambda,\beta)\ a_w\ s_w^3 \text{ Watts}$$

where ρ is the air density, s_w the wind speed, a_w is the area covered by the rotor of the wind turbine, $a_w = \pi r^2$ where r= radius of the blade, Cp is the power conversion coefficient which is the function of both tip speed ratio, λ, and blade pitch angle, β. By controlling the blade pitch angle (β), the wind turbines can extract more wind energy within the wide range area of wind speed. The tip speed ratio is defined as follows:

$$\lambda = (\omega / s_w) * r$$

where ω is the rotational mechanical speed (rad/s). For the modeling of wind turbine, Cp (,-) can be calculated as:

$$C_p\ (\lambda,\beta) = C_1\ (\ \frac{C_2}{\lambda_i}\ -\ C_3\beta - C_4\ )e^{\frac{-C_5}{\lambda_i}} - C_6\ \lambda$$

Where:

$$\lambda_i = \left[\frac{1}{\lambda + 0.08\beta} - \frac{0.035}{\beta^3 + 1}\right]^{-1}$$

The coefficients from c1 to c6 are considered as follows: C_1 = 0.5176, C_2 = 116, C_3 = 0.4, C_4 = 5, C_5 = 21, AND C_6 = −0.0068.

The basic diagram of DFIG with its two converters (RSC and grid-side converter (GSC)) is shown in Figure 3(a). The RSC and GSC are basically based on Voltage-source converter (VSC), and these two converters have the capability to transfer both active and reactive power in both directions (AC/DC/AC) autonomously (Li et al., 2012). A DC link capacitor is connected

between RSC and GSC to keep variations of the Voltage within a small range.

B. Rotor Side Controlling System:

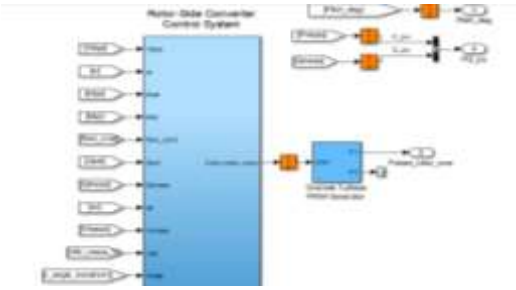

Fig. 3 Rotor Side Converter control block

RSC uses two PI controllers as shown in figure with gain K_p= 2 and K_i = 1.The Voltage vector equation and flux vector equation for RSC can be found as:

$$\overrightarrow{V_r} = r_r\overrightarrow{I_r} + \frac{d\overrightarrow{\psi_r}}{dt} - j\omega\overrightarrow{\psi_r}$$

$$\overrightarrow{\psi_r} = L_m\overrightarrow{I_s} + L_r\overrightarrow{I_r}$$

where in equations (5) and (6), V_r is the rotor-side Voltage; I_r is the current of the rotor; r_r is the rotor winding resistance; ψ_r is the flux vector for rotor; L_m is the magnetizing inductance; I_s is is the current of the stator; L_r is the rotor windings self-inductance; and finally, r and s are the rotor and stator subscripts, respectively.

The rotor self-inductance (L) r can be defined.

$$L_r = L_m + L_{lr}$$

where Llr is the leakage inductance for rotor.

In RSC, the idr and irq are processed with the help of PI controllers, and give the Voltages of v′rd and v′qr , respectively,and it is defined in equations (8) and (9)

$$V'_{dr} = r_r I_{dr} + \sigma L_r \frac{dI_{dr}}{dt}$$

$$V'_{qr} = r_r I_{qr} + \sigma L_r \frac{dI_{qr}}{dt}$$

where d and q represent the axis component subscripts, and σ is the leakage factor and

$\sigma = 1 - \frac{L_m^2}{L_s L_r}$ and equivalent to $L_0 = \frac{L_m^2}{L_s}$

In order to ensure the decent tracking of the dq axis current, in RSC controller, the compensation terms are added to $V'_{dr}$and V'_{qr} to obtain the reference Voltages ($V^*_{dr}$and V^*_{qr}), which are defined in the below equations:

$$V^*_{dr} = V'_{dr} - \omega_{slip}\sigma L_r I_{qr}$$

$$V^*_{qr} = V'_{qr} + \omega_{slip}(L_m I_{ms} + \sigma L_d I_{dr})$$

where in equations (10) and (11), ω_{slip} is the slip, and it is defined as $\omega_{slip} = \omega_s - \omega_r$.

The pulses are generated through the PWM generator after calculation of reference for the insulated-gate bipolar transistor (IGBT). They are then fed to the control bridges on the rotor side in Mat lab/ Simulink as gate pulses.

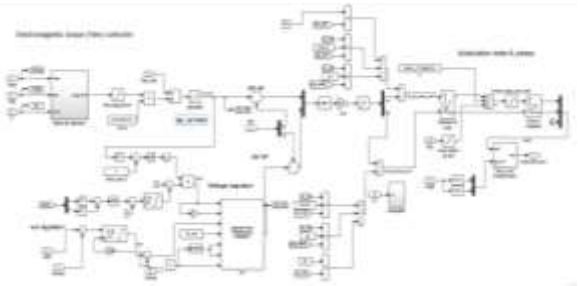

Fig. 4 Rotor Side Controlling System

C. Grid Side Controlling System:

The main purpose of the GSC is to keep fixed DC link Voltage and to keep a constant power factor. To achieve this goal the vector control method is used. In DFIG, the GSC ensures balanced power energy on the both sides of the DC link capacitor by maintaining the DC link Voltage.

In order to design the GSC, two series PI controllers are used in this research work. The gain parameter values of the GSC controller are K_p= 0.84 and K_i = 5. The GSC controller is made up of a universal bridge converter in MATLAB/ SIMULINK with snubber resistance 1e3 ohms and uses IGBT as the power electronic device. The IGBT uses gate pulses as controlling signals.

It uses the DC link Voltage v_{dc} and the reactive power (Q) s from the rotor line as inputs and sends the desired signal with the processing of the PI controller and carrier frequency of the GSC controller.

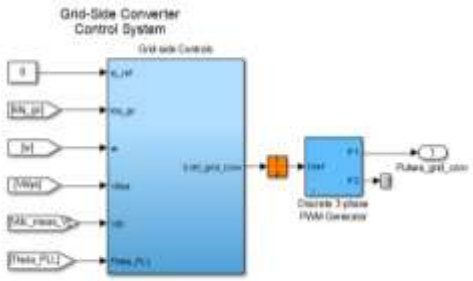

Fig. 5 Grid Side Converter control block

The stator Voltage is determined by the grid as the stator windings of the DFIG are directly connected to the grid. The Voltage and flux vector equations for GSC can be found in equations (12) and (13)

$$\overrightarrow{V_s} = r_s\overrightarrow{I_s} + \frac{d\overrightarrow{\psi_s}}{dt}$$

$$\overrightarrow{\psi_s} = L_s\overrightarrow{I_s} + L_m\overrightarrow{I_r}$$

where in equations (11) and (12), V_s is the stator side Voltage; I_r is the current of the rotor; r_s is the stator winding resistance; ψ_s is the flux vector for stator; I_s is the current of the stator; L_m is the magnetizing inductance; L_s is the stator

Windings self-inductance; and finally, r and s are the rotor and stator subscripts, respectively.

The stator self-inductance can be defined as:

$$L_s = L_m + L_{ls}$$

L_{ls} is the leakage inductance for stator

In GSC, the d-axis reference component is associated with the grid Voltage angular position α_s. As the grid Voltage amplitude is constant, V_{cq} is zero and V_{cd} is constant. The active power and reactive power will be proportional to the I_{cd} and I_{cq} , respectively.

The converter active power flow (P_{con})and the reactive power (Q_{con}) are defined in equations (15) and (16), respectively,which demonstrated the real and reactive powers from the GSC, which are controlled by I_{cd} andI_{cq}current components, respectively

$$P_{con} = 3\left(V_{cd}I_{cd} + V_{cq}I_{cq}\right) = 3V_{cd}I_{cd}$$

$$Q_{con} = 3\left(V_{cd}I_{cq} + V_{cq}I_{cd}\right) = 3(V_{cd}I_{cd})$$

where in equations (15) and (16), d, q, and con represent the axis component subscripts and converter value subscript, respectively.

In order to appreciate the decoupled control, the similar compensation also introduced in equations (17) and (18) as shown in equations (10) and (11)

$$V_{cd}^{*} = V'_{cd} + (\omega_e I_{cd} + V_d)$$

$$V_{cq}^{*} = -V'_{cq} - \left(\omega_e I_{cq}\right)$$

where V_{cd}* and V_{cq}* represent the reference Voltages, respectively.

After calculating the reference Voltages, inverse-park transformation is used in order to give the appropriate three phase Voltage ($v_{c\,abc}$ *) to the final PWM pulse generator for the GSC converter.

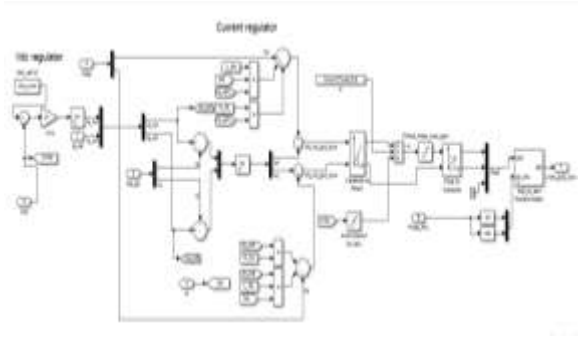

Fig. 6 Grid Side Controlling System

Required value for modulation index "m" to obtain 1 pu generated Voltage by the converter (Both RSC and GSC) is given by

m = Vnom * 2*sqrt(2/3) / vdc ,

Where Vnom = RMS ph-ph nominal Voltage

D. SFCL Configuration

DC Resistive Type SFCL: In the DC resistive SFCL, for positive half cycle of the electrical frequency line current I_L will flow through the diode D1, resistor R_{SC}, inductor L_{SC} and then through diode D4, Thus the path of the line current for this case becomes

D1 → R_{SC} → L_{SC} → D4

For negative half of line frequency the line current I_L will flow through the diode D3, resistor R_{SC}, inductor L_{SC} and then through

the diode D2, Thus the path of the line current for this case becomes

D3 ⟶ R_{SC} ⟶ L_{SC} ⟶ D2

Due to this, the current (I_{SFCL}) flowing through the superconducting coil is unidirectional. This helps minimise the loss across the coil, L_{SC}. Although there are some power losses across the rectifier diodes, it is reported that using the DC resistive SFCL provides better system efficiency, even when considering these losses

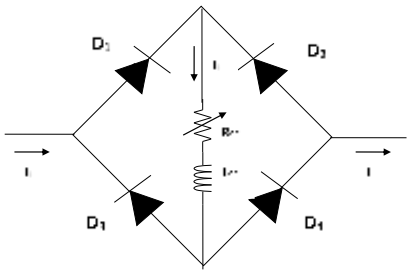

Fig. 7 Resistive Type SFCL Design

When a fault occurs line Voltage, line current, active power as well as reactive power are effected. The variable resistor R_{sh} can be modeled in order to prevent the line Voltage V_L form getting zero and preventing the system from getting detached from the bus B1 as shown in figure 1. The current during the fault is dissipated in the R_{sh} hence keeping the Voltage deviation minimum.

The DC resistive SFCL is designed in such a way that the magnitude of quench resistance varies exponentially from 0.0 to 2.0 pu. Generally in DC resistive SFCL, the resistance value of Rc is kept zero during the normal operation. During a fault, a value of quenched resistance (R_{sh}) = 0 65 pu is considered in this article to compare the transient stability performances among the series compensators. The main advantage of using the DC resistive SFCL is that no additional controller is required to change from the non-superconducting state to superconducting states.

E. Proposed Design Of IGBT-Bridge-Type SFCL

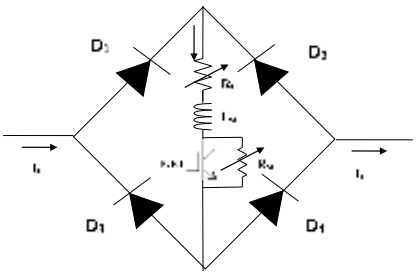

Fig. 8 Proposed SFCL Design

IGBT is used as a switch whose operation and switching will depend on the acceptable reference Voltage $V_{ref.}$ at bus terminal B1. During normal operation the bus Voltage V_{B1} is at acceptable limit and hence the control of the gate signal of IGBT will close the circuit. As soon as the V_{B1} reaches acceptable reference Voltage the IGBT gate signal pushes gate to a low state causing the IGBT to become open circuited. The variable resistor R_{SC} is shunted causing the current to flow through it limiting its value to permissible reference current I_{ref} or below it.

F. Operation of proposed design:

- During normal operation, the semiconductor IGBT switch is closed and the dc current (I_{B1})is flowing through the IGBT switch. The current (I_{B1}) is continuously compared with the preset permissible reference current (I_{ref}) for both normal and transient conditions.
- The comparator output pulse is set in such a way that if the dc current I_{B1} crosses slightly higher than preset permissible reference current I_{ref} , then the output pulse of the comparator becomes high.
- However, when the Voltage at PCC (V) pcc just reaches the predefined maximum acceptable reference Voltage (V $_{ref}$), the output pulse of the comparator becomes low. Based on the comparator signals, the logical control gives an appropriate IGBT gate control signal.
- In the event of fault, the dc current (I_{B1}) becomes greater than the I_{ref}, and after that, the controller circuit detects the fault, and the controller of the IGBT-Bridge-Type SFCL forces the IGBT gate signal to move to a low state, which opens the IGBT switch.
- After opening the IGBT switch, the high impedance of shunt path (R_{sh})is connected to the faulted, limiting the fault current instantaneously.

Another control parameter is needed to turn on the IGBT switch and return to the normal operation. After a fault, when the IGBT

switch is off, terminal Voltage control is very important to maintain the system transient stability. Therefore, to turn on the IGBT switch, the PCC Voltage (V_{B1}) and the predefined reference Voltage (V_{ref})are considered in this article because our main aim is to maintain the Voltage profile (±0.1 pu) at the B1.

How long the parallel path (R_{sh}) of the IGBT-Bridge-Type SFCL circuit will remain connected in series with the line is decided by comparison between the predefined maximum permissible reference Voltage V_{ref} and the B1 Voltage V_{B1} . The value of V_{ref} is set to 0.90 pu of the nominal value.

When V_{B1} is slightly greater than the V_{ref} , the controller forces the IGBT gate signal move to a higher state, which makes the IGBT switch turn on. As the IGBT switch is on, the shunt path is withdrawn from the operation, and normal operation of the system returns and continues.

A novel concept of an SFCL acting as a rectifier-type SFCL in normal conditions and as a resistive-type SFCL, IGBT-Bridge-type SFCL during both symmetrical and asymmetrical fault is discussed. The deviation of Voltage has considerably reduced in both case 1 and case 2 as compared to case 1 in which SFCL has not been used. This is due to reduction in fault current at the bus terminal. The fig 4.8 shows the complete DFIG based model using SFCL.

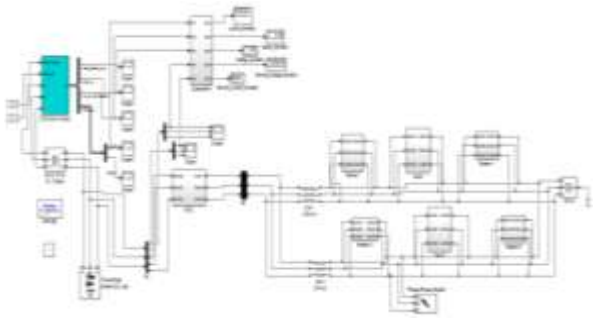

Fig. 9 Model using Resistive type SFCL

Wind turbines using a doubly-fed induction generator (DFIG) consist of a wound rotor induction generator and an AC/DC/AC IGBT-based PWM converter modeled by Voltage sources. The stator winding is connected directly to the 50 Hz grid while the rotor is fed at variable frequency through the AC/DC/AC converter. The DFIG technology allows extracting maximum energy from the wind for low wind speeds by optimizing the turbine speed, while minimizing mechanical stresses on the turbine during gusts of wind. In this model the wind speed is maintained constant at 14 m/s.

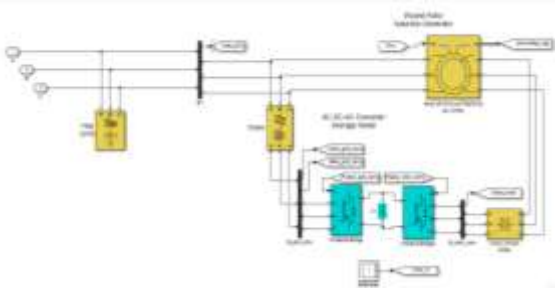

Fig. 10 DFIG MATLAB model using two Universal Bridges

The Universal Bridge block implements a universal three-phase power converter that consists of up to six power switches connected in a bridge configuration. First one is acting as rectifier and second as inverter model. It uses forced commutated devices like IGBT forming three bridge arms. The Snubber Resistance is kept to be 1000 ohms. The snubber capacitance, in farads (F) is set to inf to get a resistive snubber with internal resistance of the selected device 1 x 10^{-3} ohms. Pulses to the grid side converter and rotor side converter is provided individually by a controlling system as shown in figure 4. Discrete 3-phase PWM Generator are used to generate pulses. Sampling time (Ts) is taken to be 5.000 x 10^{-3}.

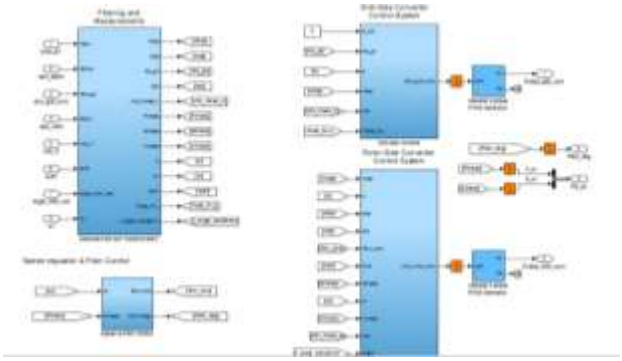

Fig. 11 Wind turbine Control system

CASE 1:

The DFIG model is designed without any SFCL. It will show the following output when it is simulated for 2 seconds in MATLAB / SIMULINK

Power Deviation = 0.0004936 %

Speed Deviation = 0.02 %

Terminal Current deviation = 0.0004663 %

Terminal Voltage deviation = 1.123 e $^{-8}$ %

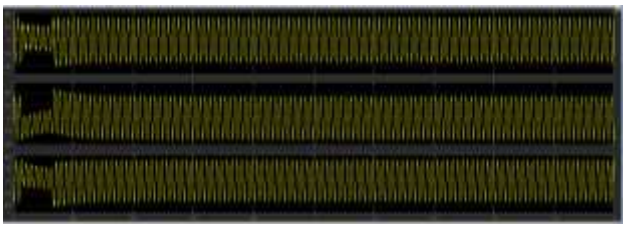

Fig. 12 Current Waveform of DFIG model without using SFCL

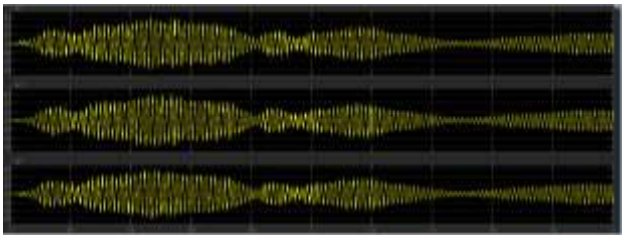

Fig. 13 Voltage Waveform in DFIG model without using SFCL

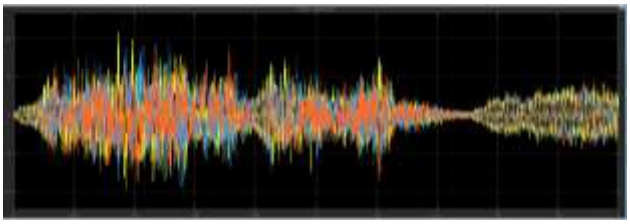

Fig. 14 DFIG stator current in case 1

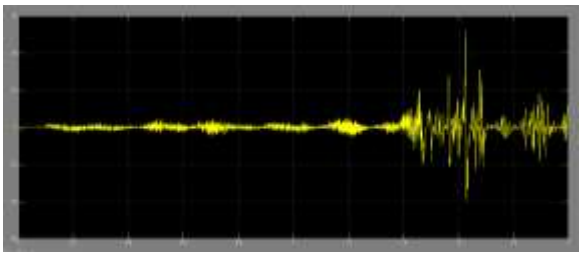

Fig. 15 Active Power P of DFIG model in p.u in case 1

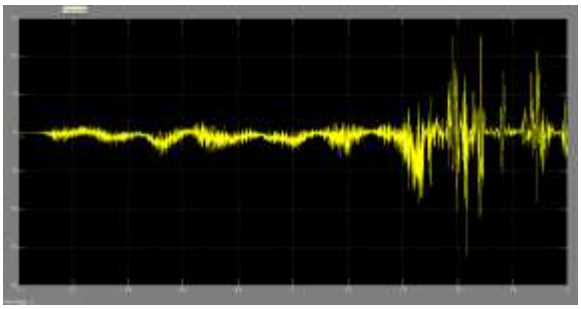

Fig. 16 Reactive Power Q of DFIG model in p.u in case 1

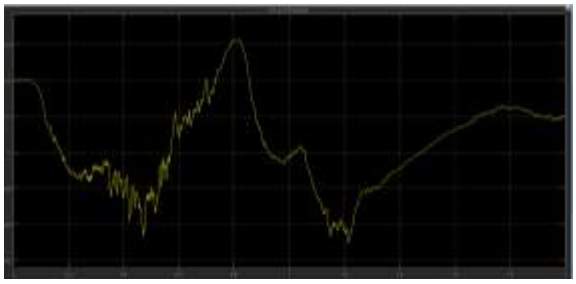

Fig. 17 Rotor Speed in of DFIG in p.u in case 1

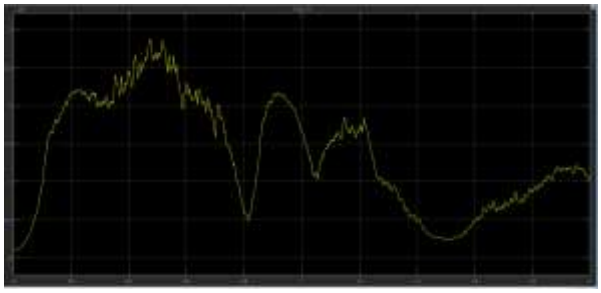

Fig. 18 VDC output from DFIG when simulated for 2 seconds in case 1

CASE II:

The design of resistive SFCL is Shown in fig. It will show the following output when it is simulated for 2 seconds in MATLAB / SIMULINK

Power Deviation = 0.0004936 %

Speed Deviation = 0.02 %

Terminal Current deviation = 0.0004663 %

Terminal Voltage deviation = 1.123 e $^{-8}$ %

The graphical output of terminal Voltage, terminal current, rotor speed, V_{DC} output from DFIG model and values of active as well as reactive power using resistive type SFCL has been shown below.

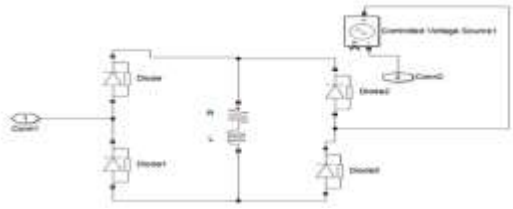

Fig. 19 The design of resistive type SFCL in MATLAB/SIMULINK

Fig. 20 Output waveform of current at the terminal B1 with resistive type SFCL

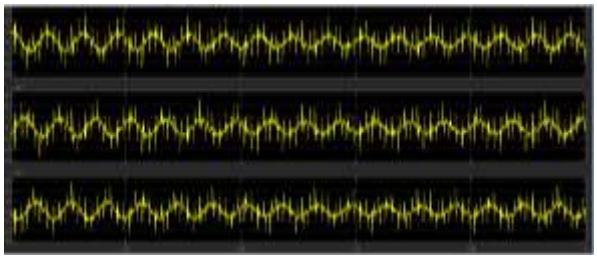

Fig. 21 Output waveform of Voltage at the terminal B1 with resistive type SFCL

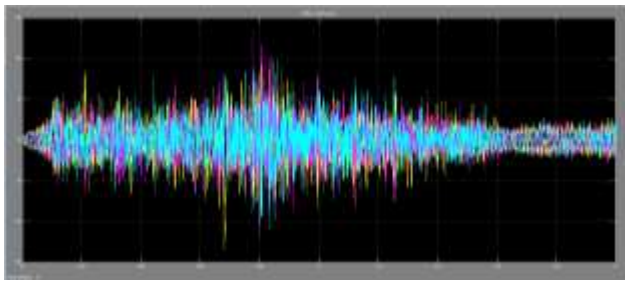

Fig. 22 DFIG stator current in case 2

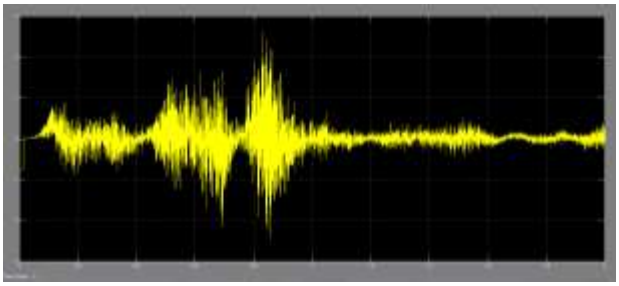

Fig. 23 Active Power P of DFIG model in p.u in case 2

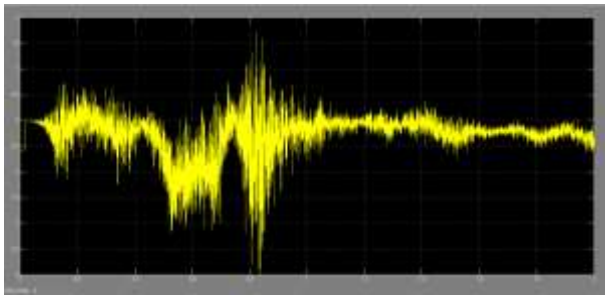

Fig. 24 Reactive Power Q of DFIG model in p.u in case 2

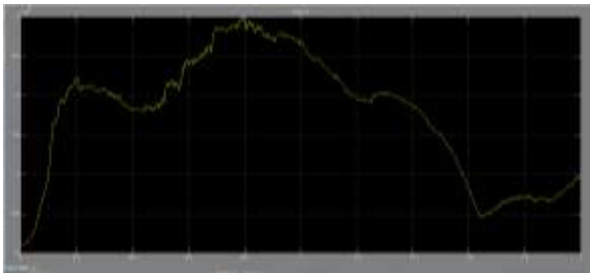

Fig. 25 VDC output from DFIG when simulated for 2 seconds in case 2

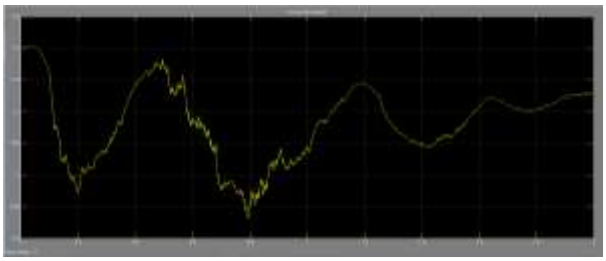

Fig. 26 Rotor Speed in of DFIG in p.u case 2

Case III :

The proposed design of IGBT-bridge-type SFCL in MATLAB/SIMULINK is Shown in fig.

It will show the following output when it is simulated for 2 seconds in MATLAB / SIMULINK

Power Deviation = 0.0004936 %

Speed Deviation = 0.02 %

Terminal Current deviation = 0.0004663 %

Terminal Voltage deviation = 1.123 e $^{-8}$ %

The graphical output of terminal Voltage, terminal current, rotor speed, V_{DC} output from DFIG model and values of active as well as reactive power using IGBT-bridge-type SFCL has been shown below.

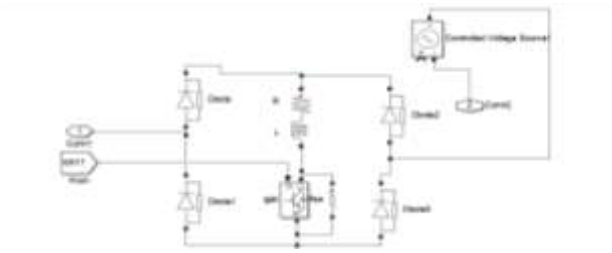

Fig. 27 The design of IGBT-bridge-type SFCL in MATLAB/SIMULINK

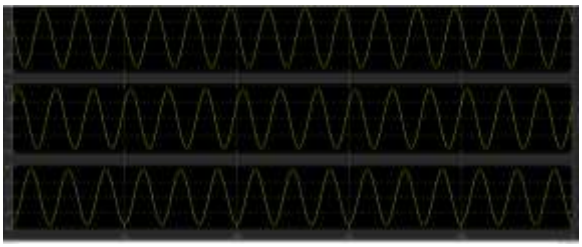

Fig. 28 Current waveform of DFIG system with proposed SFCL

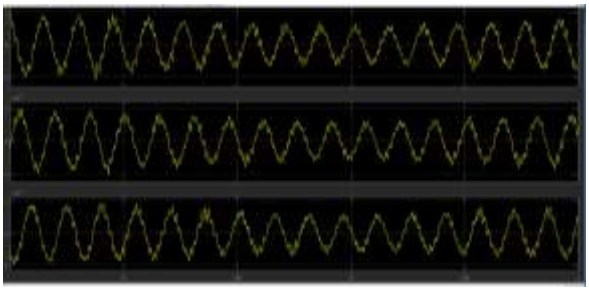

Fig. 29 Voltage waveform of DFIG system with proposed SFCL

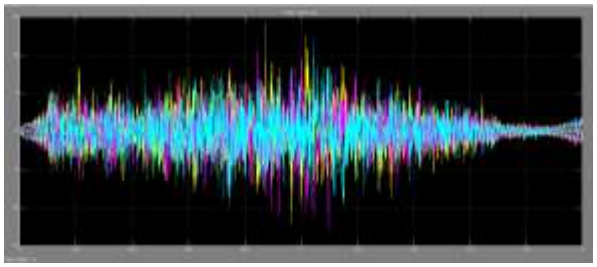

Fig. 30 DFIG stator current in case 3

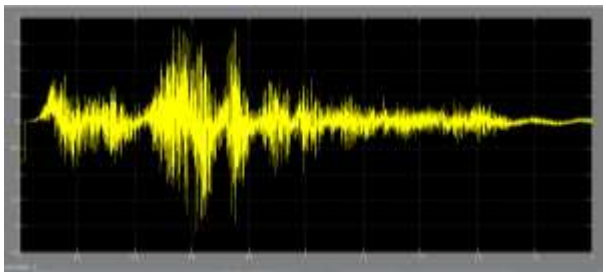

Fig. 31 Active Power P of DFIG model in p.u in case 2

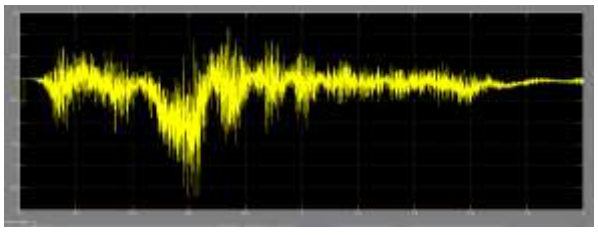

Fig. 32 Reactive Power Q of DFIG model in p.u in case 3

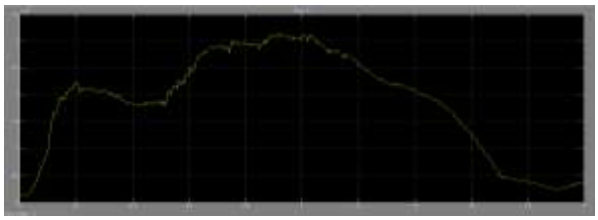

Fig. 33 VDC output from DFIG when simulated for 2 seconds in case 3

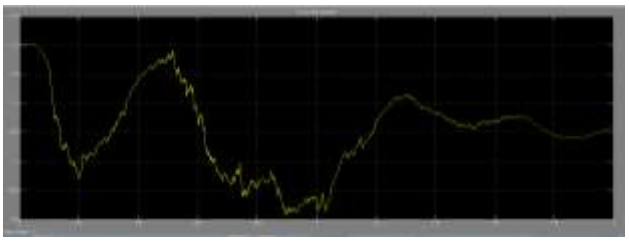

Fig. 34 Rotor Speed in of DFIG in p.u in case 3

V. RESULTS

The comparison of the DFIG model without using any controller, with DC resistive controller and

DFIG – Bridge Type SFCL has been shown below:

The model is being simulated for 0.5, 1, 1.5, 2 seconds. The corresponding values of power deviation, terminal Voltage deviation, current deviation and speed deviation has been recorded and plotted against time axis.

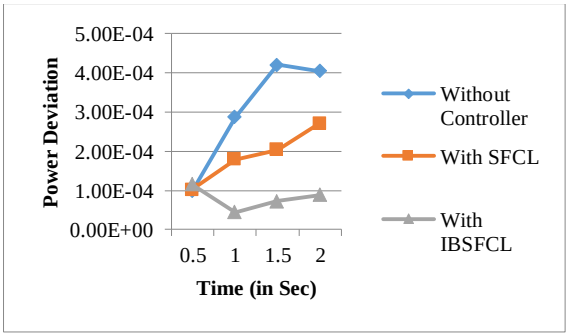

Fig. 35 Power Deviation in three cases

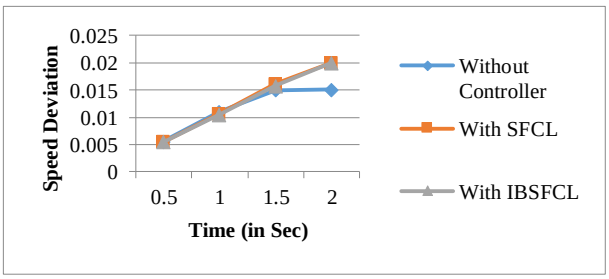

Fig. 36 Speed Deviation in three cases

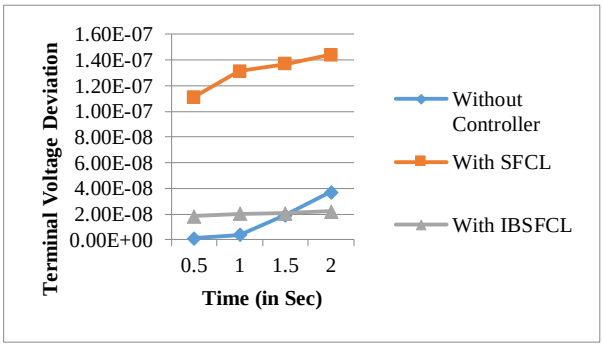

Fig. 37 Terminal Voltage Deviation in three cases

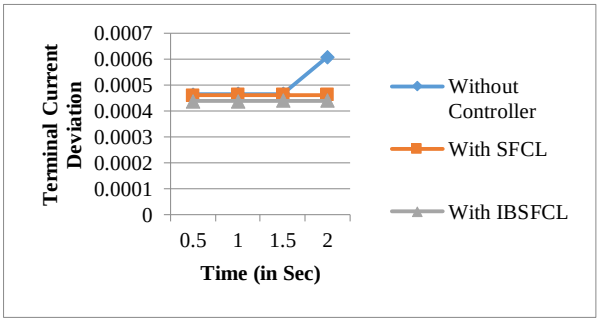

Fig. 38 Terminal Current Deviation in three cases

Table 1 Comparison of various parameters when model is simulated for 2 seconds

Parameters	Without Controller	With SFCL	With IBSFCL
Power Deviation	0.0004037	0.0002712	8.90E-05
Terminal Voltage Deviation	37.1E-08	14.4E-08	2.22E-08
Terminal current deviation	0.0006081	0.0004624	0.0004401
Speed Deviation	0.01508	0.02	0.02

VI. CONCLUSION

This study proposes the use of IGBT-bridge-Type SFCL to improve the transient stability of a DFIG based wind power system. From the simulation results, the following assessments can be noted:

(i) The proposed SFCL design with gated IGBT (IGBT-bridge-Type SFCL) is able to enhance the transient stability of the DFIG system for both the symmetrical and asymmetrical faults more efficiently than the DC Resistive type SFCL.

(ii) The values of Voltage deviation at the bus terminal is 8.223 e^{-8} % for IGBT-bridge-Type SFCL and it is 14.4 e^{-8} % for Resistive type SFCL when the DFIG model is simulated for 2 seconds.

(iii) The huge Voltage sag has been considerably reduced by reduction of high level of current to 0.0004401 % in IGBT-bridge-Type SFCL from 0.0004624% in resistive type SFCL.

(iv) Huge Voltage sag and high levels of fault current are significantly suppressed by the IGBT-bridge-Type SFCL.

Thus proposed SFCL has caused significant improvement in transient stability keeping the deviation in active and reactive power during faults to minimum level. The use of fast switching, forced commutated device like IGBT shunted with a variable resistance, can improve the performance of the system significantly during abnormal conditions.

Further the enhancement of this design can lead to a better output and can make this system to work for low Voltage ride through LVRT also.

REFERENCES

[1] M. A. Chowdhury, N. Hosseinzadeh, M. M. Billah, and S. A. Haque, "Dynamic dfig wind farm model with an aggregation technique," in International Conference on Electrical Computer Engineering (ICECE 2010), pp. 330–333, Dec 2010.

[2] J. Wang, M. Han, Z. Wang, S. Wei, and Y. Gu, "Lumping and electromechanical transient modeling of large-scale wind farm," in 2014 International Conference on Power System Technology, pp. 2840–2845, Oct 2014.

[3] Y. Lei, A. Mullane, G. Lightbody, and R. Yacamini, "Modeling of the wind turbine with a doubly fed induction generator for grid integration studies," IEEE Transactions on Energy Conversion, Vol. 21, pp. 257– 264, March 2006.

[4] Z. Zhao, P. Yang, Z. Xu, and X. Yin, "Dynamic equivalent modeling of wind farm with double fed induction wind generator based on operating data," in 2013 5th International Conference on Power Electronics Systems and Applications(PESA), pp. 1–6, Dec 2013.

[5] M. Rosyadi, A. Umemura, R. Takahashi, J. Tamura, N. Uchiyama, and K. Ide, "A new simple model of wind turbine driven doubly-fed induction generator for dynamic analysis of grid connected large scale wind farm," in 3rd Renewable Power Generation Conference (RPG 2014), pp. 1–6, Sept 2014.

[6] D. J. Kim, Y. H. Moon, and H. K. Nam, "A new simplified doubly fed induction generator model for transient stability studies," IEEE Transactions on Energy Conversion, Vol. 30, pp. 1030–1042, Sept 2015.

[7] D. Schwanz, M. Bollen, A. Larsson, and H. Kocewiak, "Harmonic mitigation in wind power plants: Active filter solutions," in 2016 17th International Conference on Harmonics and Quality of Power (ICHQP), pp. 220–225, Oct 2016.

[8] N. Dhlamini and S. P. Chowdhury, "The impact of wind farm aggregation techniques for analyzing power system dynamics," in 2015 50th International Universities Power Engineering Conference (UPEC), pp. 1–6, Sept 2015.

[9] J. Y. Ruan, Z. X. Lu, Y. Qiao, and Y. Min, "Analysis on applicability problems of the aggregation-based representation of wind farms

considering dfigs x2019; lvrt behaviors," IEEE Transactions on Power Systems, Vol. 31, pp. 4953–4965, Nov 2016.

[10] M. Kayikci and J. V. Milanovic, "Assessing transient response of dfigbased wind plants x2014;the influence of model simplifications and parameters," IEEE Transactions on Power Systems, Vol. 23, pp. 545– 554, May 2008.